Asian Journal of Chemistry; Vol. 33, No. 8 (2021), 1905-1910

ASIAN JOURNAL OF CHEMISTRY

https://doi.org/10.14233/ajchem.2021.23201

Structural, Electronic, Molecular Orbital Analysis and Charge Distributions on Nitrate Salt of Guanidine through DFT and TD-DFT Methods

S. THANGARASU[1,2,*], V. SIVA[1,2], A. SHAMEEM[1,2], A. MURUGAN[1,2], S. ATHIMOOLAM[3] and S. ASATH BAHADUR[1,2]

[1]Department of Physics, School of Advanced Sciences, Kalasalingam Academy of Research and Education, Krishnankoil-626126, India
[2]Condensed Matter Physics Laboratory, International Research Centre, Kalasalingam Academy of Research and Education, Krishnankoil-626126, India
[3]Department of Physics, University College of Engineering (Affiliated to Anna University), Nagercoil- 629004, India

*Corresponding author: E-mail: sthangarasu@gmail.com

Received: 9 March 2021; *Accepted*: 10 June 2021; *Published online*: 26 July 2021; AJC-20444

Guanidinium nitrate, a non-linear optical material has been systematically studied through quantum chemical (density functional theory and Hartree Fock) methods. Studies on Mulliken charge, Frontier molecular orbitals (FMOs) and hyperpolarizability analyses have been performed. The Mulliken population analyses were carried out for the optimized molecular geometry by HF and B3LYP methods with 6-311++G(d,p) levels. The molecular orbital parameters of guanidinium nitrate have been calculated by FMO analysis. Frontier molecular orbital (FMO) analysis indicates the electron delocalization on the guanidinium nitrate and also its low value of energy gap indicates electron transfer. Optical property has been investigated by time-dependent density functional theory (TD-DFT) calculation. The second-order hyperpolarizability value of the ion pairs is much greater than urea, which confirms the good NLO nature of guanidinium nitrate.

Keywords: Density functional theory, TD-DFT, Mulliken charge distributions, HOMO-LUMO, Non-linear optics.

INTRODUCTION

Evolution of non-linear optical crystals has marked remarkable achievements in the optics fields. Organic or inorganic single crystals play an essential responsibility in optical device fabrication required to the multifaceted property such as high non-linear efficiency, architectural flexibility, good mechanical strength, rapid response and easiness of fabrication [1]. In general, extensive investigation going on organic NLO materials for the reason of their high non-linear optical coefficients, large hyperpolarizability, large optical non-linearity [2], easy to prepare, low production cost [3] and rapid electro-optic response compared to inorganic counterparts [4]. Organic molecules that include cationic and anionic spices with the classical hydrogen bonding interactions have high non-linearity and exhibit non-linear optical properties. Guanidine is widely embedded in a range of spectrum-wide supramolecular recognition processes such as in organic, chemistry, medicine with special interest encouraged by their potential non-linear optics applications [5].

Guanidine, a cation of Lewis base with six potential donor sites which may readily be protonated by organic and inorganic acids. As a resonance stabilized cation, assorted structures could have prevailed from the choice of anchoring anions and thereby tunable to a spectrum of applications such as opto-electronic materials, biological, medicinal, energy harvesting, *etc*. guanidinium architecture family include guanidinium L-tartrate monohydrate [6], guanidinium 4-aminobenzoate [7], guanidinium 4-nitrobenzoate [8], guanidinium L-glutamate [9], guanidinium cinnamate [10], guanidinium propionate [11], guanidinium 4-nitrophenolate [12] and guanidinium perchlorate [13] in the literature. In the trail of this article, an attempt has been performed for developing an amino-rich material intrinsically more hydrogen bonds with possible π-interactions. The molecular orbital, population, hyperpolarizability values were calculated and discussed.

COMPUTATIONAL METHODS

Quantum chemical calculations is performed from the crystallographic data with HF and DFT/B3LYP with 6-311++G

(d,p) levels using GAUSSIAN 09W software package [14]. For quantum chemical studies, the input of crystallographic information file (CIF) is available with the CCDC deposition (CCDC No.: 1205934). Initially, the HF analysis, adopting the 6-311++G(d,p) basis set were carried out and then the DFT using the Becke-3-Lee-Yang-Parr (B3LYP) supplemented with the standard 6-311++G(d,p) basis set. The optimized geometrical parameters were compared with experimental data [15-18]. Analysis of Frontier molecular orbital (FMO) is another approach to studying the transfer of molecular charge. Gauss View 05 [19] was used to visualize the optimized structure, molecular electrostatic potential surface (MEP), FMO of the compound. NLO parameters have also been calculated.

RESULTS AND DISCUSSION

Molecular structure analysis: Guanidinium molecule is occupied with eight units of the ionic pairs in the unit cell in the monoclinic crystal system [20]. The optimized structure of guanidinium nitrate is shown in Fig. 1. The optimized C–N bond length varies from 1.309 to 1.353 Å and 1.309 to 1.372 Å in HF and DFT methods, respectively. These optimized bond distances are different from that of XRD due to the fact that the theoretical prediction was done for the molecule in the gaseous phase, whereas the experimental results were carried out in the solid crystalline state. Because of methyl group positional disorder, the C–C single bond distance varies slightly from the reported value. The nitrate moiety and the planar guanidinium moiety are oriented at an angle of 84.7(2)º to each other. The optimized geometrical parameters is presented in Table-1.

Mulliken charge analysis: Population analysis has an important part in the molecular system since atomic charges affect dipole moment, polarizability and electronic structure. The atomic charge distribution of guanidinium nitrate is shown in Fig. 2 and the Mulliken charge values are given in Table-2. The charge distribution of guanidinium nitrate shows that the nitrogen N8 atom (-0.708 e in HF and -0.529 e in DFT) has higher electronegativity than other atoms because the carbon atom is attached with two electropositive hydrogen atom (H9

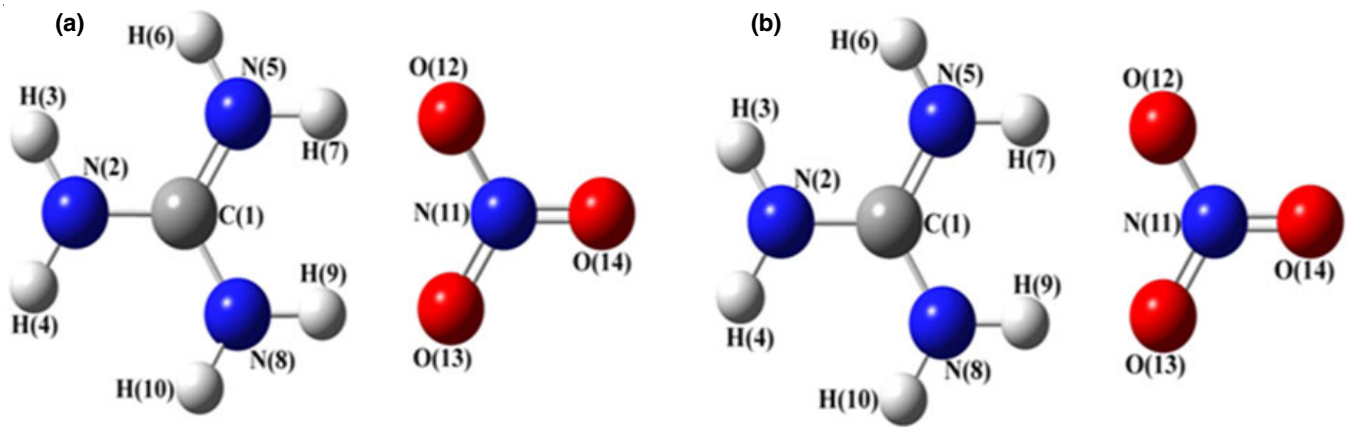

Fig. 1. Optimized structure of guanidinium nitrate (a) DFT and (b) HF levels

TABLE-1
IMPORTANT OPTIMIZED GEOMETRICAL PARAMETERS OF GuN

Bond length (Å)	HF	DFT	Bond angle (°)	HF	DFT	Torsional angle (°)	HF	DFT
C(1)–N(2)	1.345	1.3617	N(2)–C(1)–N(5)	119.94	120.59	N(5)–C(1)–N(2)–H(3)	11.03	6.25
C(1)–N(5)	1.312	1.3242	N(2)–C(1)–N(8)	119.92	119.85	N(5)–C(1)–N(2)–H(4)	168.06	159.00
C(1)–N(8)	1.312	1.3261	N(5)–C(1)–N(8)	120.14	119.55	N(8)–C(1)–N(2)–H(3)	-169.68	-174.83
N(2)–H(3)	0.993	1.0067	C(1)–N(2)–H(3)	119.73	119.43	N(8)–C(1)–N(2)–H(4)	-12.65	-22.08
N(2)–H(4)	0.993	1.0071	C(1)–N(2)–H(4)	119.71	119.03	N(2)–C(1)–N(5)–H(6)	2.20	-6.84
N(5)–H(6)	0.992	1.0064	H(3)–N(2)–H(4)	116.66	116.02	N(2)–C(1)–N(5)–H(7)	174.48	169.83
N(5)–H(7)	1.023	1.0598	C(1)–N(5)–H(6)	120.44	120.57	N(8)–C(1)–N(5)–H(6)	-177.09	174.23
O(12)···H(7)	1.713	1.6069	C(1)–N(5)–H(7)	119.93	119.41	N(8)–C(1)–N(5)–H(7)	-4.81	-9.10
N(8)–H(9)	1.023	1.0568	H(6)–N(5)–H(7)	119.18	119.94	N(2)–C(1)–N(8)–H(9)	-178.21	178.74
N(8)–H(10)	0.992	1.0065	C(1)–N(8)–H(9)	120.06	119.21	N(2)–C(1)–N(8)–H(10)	-1.72	-10.60
O(13)···H(9)	1.711	1.62	C(1)–N(8)–H(10)	120.53	120.17	N(5)–C(1)–N(8)–H(9)	1.08	-2.33
N(11)–O(12)	1.237	1.2775	H(9)–N(8)–H(10)	119.32	119.96	N(5)–C(1)–N(8)–H(10)	177.57	168.34
N(11)–O(13)	1.237	1.2762	N(8)–H(9)···O(13)	177.01	176.72	C(1)–N(5)···O(12)–N(11)	10.72	25.58
N(11)–O(14)	1.186	1.219	O(12)–N(11)–O(13)	118.11	118.40	H(6)–N(5)···O(12)–N(11)	-178.07	-159.61
			O(12)–N(11)–O(14)	120.95	120.75	C(1)–N(8)–H(9)···O(13)	-19.81	-45.94
			O(13)–N(11)–O(14)	120.94	120.85	H(10)–N(8)–H(9)···O(13)	163.66	143.37
			H(7)···O(12)–N(11)	123.45	120.76	N(8)–H(9)···O(13)–N(11)	27.38	67.96
			H(9)···O(13)–N(11)	123.30	121.25	O(13)–N(11)–O(12)···H(7)	-3.99	-9.43
						O(14)–N(11)–O(12)···H(7)	176.01	170.56
						O(12)–N(11)–O(13)···H(9)	-3.62	-9.40
						O(14)–N(11)–O(13)···H(9)	176.38	170.62

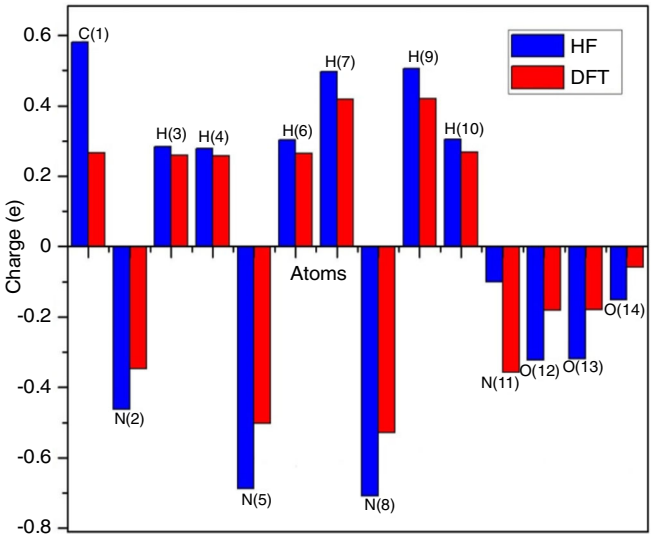

Fig. 2. Atomic charges of guanidinium nitrate

TABLE-2
ATOMIC CHARGES FOR OPTIMIZED GUANIDINIUM NITRATE

Atoms	HF	DFT	Atoms	HF	DFT
C(1)	0.580	0.266	N(8)	-0.708	-0.529
N(2)	-0.463	-0.346	H(9)	0.506	0.420
H(3)	0.284	0.260	H(10)	0.305	0.268
H(4)	0.279	0.257	N(11)	-0.101	-0.358
N(5)	-0.688	-0.503	O(12)	-0.323	-0.181
H(6)	0.302	0.265	O(13)	-0.319	-0.180
H(7)	0.497	0.418	O(14)	-0.152	-0.059

& H10). The elongation of C–N bond distance due to the protonation is repeated due to electronegative repulsion between C1 and N8 atoms. This confirms the presence of N–H···O (N(8)–H(9)···O(13) intermolecular hydrogen bond in the molecular structure. In general, carbon atom attached with electronegative, the charge of carbon atom changes from negative to positive, which indicates that the delocalization of charge essentially stand up through carbon atoms.

All hydrogen atoms are found to be positive in nature. In addition, the two hydrogen atoms H9 (0.506 e and 0.420 e for HF and B3LYP methods, respectively) and H7 (0.497 e and 0.418 e for HF and B3LYP methods, respectively) have higher positive charge than the other hydrogen atoms. It is due to the fact that two hydrogen atoms are situated between a donor N atom of the cation and an acceptor O atom in the anion. Hence, it makes the N–H···O hydrogen bonds to form a dimeric ring motif in the solid crystalline state.

HOMO-LUMO analysis: Conjugated π-electrons in many organic molecules are characterized as hyperpolarizability examined by means of electronic spectroscopy, vibrational spectroscopy and quantum mechanical calculation [21]. The FMOs analysis is such as highest occupied molecular orbital (HOMO) and lowest unoccupied molecular orbital (LUMO). Chemical hardness, chemical potential and electro negativity information of guanidinium nitrate is given by these orbitals. HOMO and LUMO energies are calculated by HF/B3LYP methods with 6–311++G(d, p) basis set. Energy level diagram of molecular orbits of guanidinium nitrate is shown in Fig. 3.

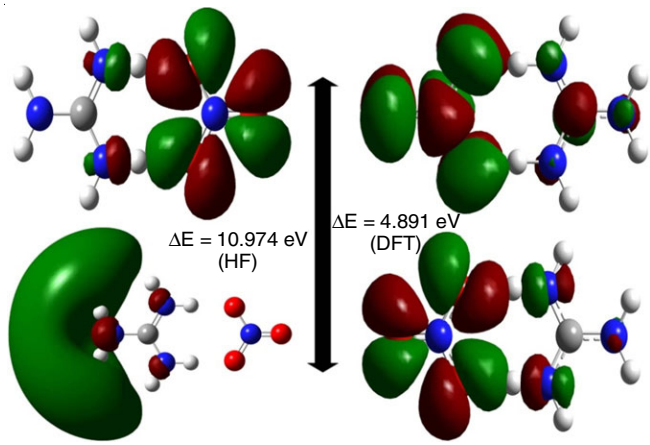

Fig. 3. Molecular energy diagram of guanidinium nitrate by (a) HF and (b) B3LYP levels

The energy difference between HOMO and LUMO analysis is called as band-gap, which is an important parameter to indicate the structure stability. The HOMO-LUMO analysis has also been used to elucidate the charge transfer phenomena within the molecule. The chemical hardness (η), electron affinity (A), electro-negativity (χ), electrophilicity index (ω), global softness (ν) and chemical potential (l) have been calculated using the HOMO and LUMO. The obtained energy values of HOMO and LUMO for the compound are -0.399 a.u and 0.003 a.u in HF level, -0.236 a.u and -0.0564 a.u in DFT level. The calculated energy gap value is 10.974/4.891 eV in HF/B3LYP methods, respectively. The calculated molecular properties of the title compound such as chemical hardness (0.201/0.089), electron affinity (-0.003/0.056), electronegativity (0.198/0.146), electrophilicity index (0.097/0.119), global softness (4.964/11.137) and chemical potential (0.399/0.236) HF/B3LYP methods, respectively. The calculated molecular orbital property of mical potential is given in Table-3. These results show that the molecule has good stability, high chemical potential, small energy gap and connected with the existence of charge transfer within the molecule and high chemical reactivity.

TABLE-3
CALCULATED ENERGY VALUES OF GUANIDINIUM NITRATE

Molecular properties	HF	DFT
HOMO	-0.399	-0.236
LUMO	0.003	-0.056
$\Delta(E_{HOMO}-E_{LUMO})$ (a.u)	0.403	0.1796
$\Delta(E_{HOMO}-E_{LUMO})$ eV	10.974	4.892
Ionization potential (I)	0.399	0.236
Electron affinity (A)	-0.003	0.056
Global hardness (η)	0.201	0.090
Global softness (ν)	4.965	11.137
Electro negativity (χ)	0.198	0.146
Chemical potential (?)	-0.198	-0.146
Global electrophilicity (ω)	0.097	0.119

Molecular electrostatic potential (MEP) surface analysis: In general, MEP is mostly used to identify the reactive behaviour of a molecule, in that negative regions should be observed as nucleophilic centers, whereas the positive sections are potential electrophilic sites. Molecular electrostatic potential

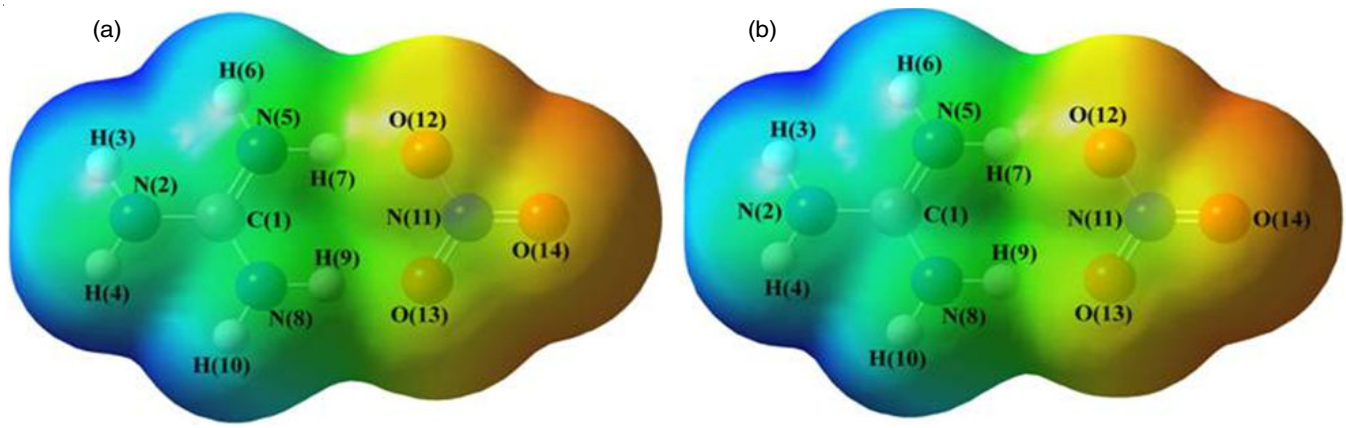

Fig. 4. MEP surface of guanidinium nitrate by (a) HF and (b) B3LYP levels

surface was investigated at HF/B3LYP with 6-311++G(d,p) methods. MEP surface images for positive and negative sites are shown in Fig. 4. The differences of the electrostatic potential at the surface are represented by different colours and the potential decreases in the order blue > green > orange > red. In the MEP surface, the region with red colour is regarded as most electronegative (electrophilic) region and the region with blue colour is most positive region, where as the bluish green colour bounded by the ring system of guanidinium nitrate is related to less positive region. The MEP map of guanidinium nitrate evidently recommends that the N and O atoms agree to the most negative (-ve) potential region. From this study, hydrogen atoms are the maximum influence of positive charges.

Electronic spectra analysis: The origin of electronic spectrum of the compound has been computed using TD-DFT method. Time-dependent density functional theory on the electronic spectrum of organic materials are usually carried out by separate calculations on the ground state and each excited state. In general, π-conjugated system are meant a molecule with a backbone in which a series of carbon atoms or heteroatoms are formed each carrying an π-atomic orbital [22,23]. The planar of molecular system, there occurs a strict difference between π-orbitals and σ orbitals (symmetric). Computed electronic spectra of guanidinium nitrate are given in Fig. 5.

The main features of the conjugated molecules is the interconnection between electronic and molecular structures. While

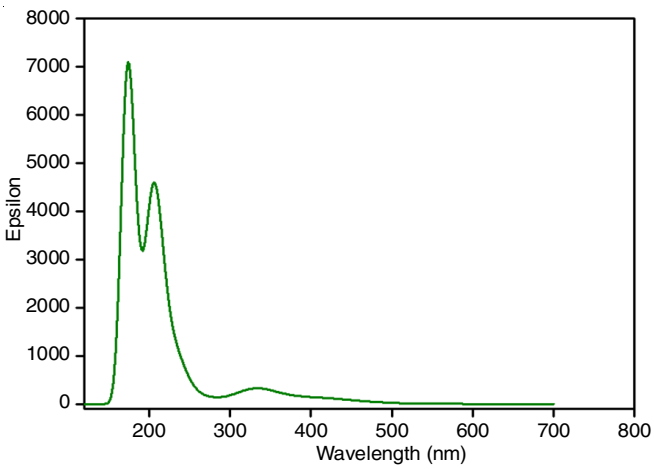

Fig. 5. Computed electronic spectrum of guanidinium nitrate

the values vary due to the various calculations and parameters active, most of the observations dispatch the weak peak at 5.92 eV to the in-plane polarized π→π* transition and the band at 6.247 eV to the out-of-plane π→π* transition. The TD-DFT computation for the interest complexes predicts strong electronic transitions located at 198 nm (Table-4). Fig. 5 shows the S_0 to S_1 transition of the compound located near the 200 nm. It is also noted that the simulated absorption spectra of the title compound exhibited maxima attributed to the π→π* (HOMO-LUMO) transitions in the range 180-320 nm [24]. Finally, the compounds under investigation could be used as optoelectronic material with intense wide absorption spectra.

TABLE-4
MAIN TRANSITION STATES, ENERGY GAP AND OSCILLATOR STRENGTH FOR THE TITLE COMPOUND

Electronic transitions	Energy gap (eV)	λ_{max} (nm)	Oscillator strength (f)
$S_0 \rightarrow S_1$	6.247	198.48	0.0209
$S_0 \rightarrow S_2$	5.920	209.43	0.0745

Non-linear optical responses: Many different challenges and issues identified in the determination of NLO properties with high accuracy. In the novel NLO materials, computational techniques are identified as a valuable method by finite-field approach. Density functional theory has been used to investigate the NLO properties of materials, computationally with quantum calculations and at the forefront of recent research, due to its importance in providing the main functions of optical parametric oscillators, optical limiting and data storage. NLO parameters such as dipole moment (μ), polarizability (α), first-order hyperpolarizability (β) and second-order hyperpolarizability (γ) values were found by using these calculated components in the following formulas [25-27] and presented in Table-5.

$$\text{Dipole moment } (\mu) = (\mu_x^2 + \mu_y^2 + \mu_z^2)^{1/2} \quad (1)$$

$$\text{Polarizability } (\alpha) = \frac{1}{3}(\alpha_{xx} + \alpha_{yy} + \alpha_{zz}) \quad (2)$$

$$\text{First-order hyperpolarizability } (\beta) = [(\beta_{xxx} + \beta_{xyy} + \beta_{xzz})^2 + (\beta_{yyy} + \beta_{yzz} + \beta_{yxx})^2 + (\beta_{zzz} + \beta_{zxx} + \beta_{zyy})^2]^{1/2} \quad (3)$$

TABLE-5
NON-LINEAR OPTICAL PARAMETERS OF GUANIDINIUM NITRATE CALCULATED BY DFT/B3LYP METHOD

Parameter	a.u	esu ($\times 10^{-24}$)	Parameter	a.u	esu ($\times 10^{-33}$)	Parameter	a.u	esu ($\times 10^{-36}$)
$?_x$	17.130	–	β_{xxx}	-178.979	-1582	γ_{xxxx}	1393.265	206.482
$?_y$	-0.647	–	β_{xxy}	-1.598	-14.125	γ_{xxyy}	255.482	37.862
$?_z$	0.405	–	β_{xyy}	-34.591	-305.75	γ_{yyyy}	206.613	30.620
M	17.147	–	β_{yyy}	-2.217	-19.596	γ_{yyzz}	50.271	7.450
α_{xx}	-45.063	-6.678	β_{xxz}	-4.785	-42.295	γ_{xxzz}	264.216	39.1567
α_{xy}	-2.417	-0.358	β_{xyz}	-1.685	-14.894	γ_{zzzz}	47.426	7.028
α_{yy}	-43.122	-6.390	β_{yyz}	1.438	12.710	γ	557.448	82.613
α_{xz}	0.834	0.124	β_{xzz}	3.973	35.117			
α_{yz}	0.845	0.125	β_{yzz}	-0.553	-4.885			
α_{zz}	-48.049	-7.120	β_{zzz}	-0.018	-0.159			
A	-45.411	-6.729	β_0	35.725	315.773			
$\Delta\alpha$	6.342	0.939						

Second-order hyperpolarizability (γ) =

$$\frac{1}{5}(\gamma_{xxxx} + \gamma_{yyyy} + \gamma_{zzzz} + 2\,\gamma_{xxyy} + 2\,\gamma_{zzyy} + 2\,\gamma_{zzxx}) \quad (4)$$

In general, the experimental method provides the information of second harmonic generation in terms of molecular level polarizability. For this reason, the second-order hyperpolarizability calculation was attempted and calculated value in the optimized structure is 82.613×10^{-36} esu, which is nearly 17 times greater than the standard urea (4.728×10^{-36} esu). Based on these results suggests that the title molecule may have non-linear optical application as a third harmonic generator [28]. Also, the large value of second-order hyperpolarizability is highly responsible for the higher non-linear optical efficiency. The larger value of hyperpolarizability and lower value of HOMO-LUMO band gap indicates the suitability of guanidinium nitrate for optoelectronic applications.

Conclusion

The structural parameters of the guanidinium nitrate were optimized at HF/DFT with B3LYP/6-311++G(d,p) levels. Computationally obtained calculated parameters are in good agreement with experimental values. The low energy gap value from molecular orbital study assists the charge delocalization in the molecule, which makes the material to be NLO active. The Mulliken charge analysis confirms the charge distribution occurs between the molecules. Molecular electrostatic potential gives the visual demonstration of the chemical reactivity of the atoms. The time dependent-density functional theory calculation for the attention complexes forecasts strong electronic transitions located at 198 nm. It is also noted that the simulated absorption spectra of the title compound exhibited maxima attributed to the $\pi \rightarrow \pi^*$ transitions in the range 180-320 nm. The nitrate salt of guanidine revealed better NLO property and are much 17 times greater than that of standard urea. These results showed that the guanidinium nitrate is a good candidate for the optoelectronic device applications.

ACKNOWLEDGEMENTS

This work was supported by the Council of Scientific and Industrial Research (CSIR) [grant No. 03(1276)/13/EMR-ll), New Delhi, India.

CONFLICT OF INTEREST

The authors declare that there is no conflict of interests regarding the publication of this article.

REFERENCES

1. D. Sajan, I.H. Joe and V.S. Jayakumar, *J. Raman Spectrosc.*, **37**, 508 (2006); https://doi.org/10.1002/jrs.1424
2. V. Siva, S. Asath Bahadur, A. Shameem, A. Murugan, S. Athimoolam and M. Suresh, *Opt. Mater.*, **96**, 109290 (2019); https://doi.org/10.1016/j.optmat.2019.109290
3. F. Helen and G. Kanchana, *J. Mat. Chem. Phys.*, **151**, 5 (2015); https://doi.org/10.1016/j.matchemphys.2014.11.064
4. V. Siva, S.S. Kumar, M. Suresh, M. Raja, S. Athimoolam and S.A. Bahadur, *J. Mol. Struct.*, **1133**, 163 (2017); https://doi.org/10.1016/j.molstruc.2016.11.088
5. P. Blondeau, M. Segura, R. Pérez-Fernández and J. de Mendoza, *Chem. Soc. Rev.*, **36**, 198 (2007); https://doi.org/10.1039/B603089K
6. P. Vivek, R.R. Kumar and P. Murugakoothan, *J. Cryst. Growth*, **412**, 40 (2015); https://doi.org/10.1016/j.jcrysgro.2014.11.042
7. T. Arumanayagam and P. Murugakoothan, *Mater. Lett.*, **65**, 2748 (2011); https://doi.org/10.1016/j.matlet.2011.05.081
8. V. Sasikala, D. Sajan, K.J. Sabu, T. Arumanayagam and P. Murugakoothan, *Spectrochim. Acta A Mol. Biomol. Spectrosc.*, **139**, 555 (2015); https://doi.org/10.1016/j.saa.2014.12.013
9. T. Arumanayagam, S. Ananth and P. Murugakoothan, *Spectrochim. Acta A Mol. Biomol. Spectrosc.*, **97**, 741 (2012); https://doi.org/10.1016/j.saa.2012.07.039
10. V. Siva, S.S. Kumar, A. Shameem, M. Raja, S. Athimoolam and S.A. Bahadu, *J. Mater. Sci. Mater. Electron.*, **28**, 12484 (2017); https://doi.org/10.1007/s10854-017-7070-8
11. S. Vadivel, A.B. Sultan, S.A. Samad, A. Shunmuganarayanan and R. Muthu, *Chem. Phys. Lett.*, **707**, 165 (2018); https://doi.org/10.1016/j.cplett.2018.07.055
12. M. Dhavamurthy, G. Peramaiyan and R. Mohan, *J. Cryst. Growth*, **399**, 13 (2014); https://doi.org/10.1016/j.jcrysgro.2014.04.013
13. M. Drozd and D. Dudzic, *Spectrochim. Acta A Mol. Biomol. Spectrosc.*, **115**, 345 (2013); https://doi.org/10.1016/j.saa.2013.06.023
14. M.J. Frisch, G.W. Trucks, H.B. Schlegel, G.E. Scuseria, M.A. Robb, J.R. Cheeseman, G. Scalmani, V. Barone, B. Mennucci, G.A. Petersson, H. Nakatsuji, M. Caricato, X. Li, H.P. Hratchian, A.F. Izmaylov, J. Bloino, G. Zheng, J.L. Sonnenberg, M. Hada, M. Ehara, K. Toyota, R. Fukuda, J. Hasegawa, M. Ishida, T. Nakajima, Y. Honda, O. Kitao, H. Nakai, T. Vreven, J.A. Montgomery Jr., J.E. Peralta, F. Ogliaro, M. Bearpark, J.J. Heyd, E. Brothers, K.N. Kudin, V.N. Staroverov, R.

Kobayashi, J. Normand, K. Raghavachari, A. Rendell, J.C. Burant, S.S. Iyengar, J. Tomasi, M. Cossi, N. Rega, J.M. Millam, M. Klene, J.E. Knox, J.B. Cross, V. Bakken, J. Jaramillo, R. Gomperts, R.E. Stratmann, C. Adamo, O. Yazyev, A.J. Austin, R. Cammi, C. Pomelli, J.W. Ochterski, R.L. Martin, K. Morokuma, V.G. Zakrzewski, G.A. Voth, P. Salvador, J.J. Dannenberg, S. Dapprich, A.D. Daniels, O. Farkas, J.B. Foresman, J.V. Ortiz, J. Cioslowski and D.J. Fox, Gaussian 09, Revision B.01. Gaussian Inc., Wallingford (2010).

15. R.G. Parr and W. Yang, Density-Functional Theory of Atoms and Molecules, Oxford University Press (1989).
16. W. Koch and M.C. Holthausen, A Chemist's Guide to Density Functional Theory, Wiley-VCH, Weinheim (2000).
17. D. Young, Computational Chemistry: A Practical Guide for Applying Techniques to Real World Situations, Wiley: USA (2001).
18. C.J. Cramer, Essentials of Computational Chemistry, Wiley: USA (2003).
19. R. Dennington, T. Keith and J. Millam, Gauss View Version 5.0.8 Semichem Inc., Shawnee Mission KS (2013).
20. A. Katrusiak and M. Szafrañski, *Acta Crystallogr. C*, **50**, 1161 (1994); https://doi.org/10.1107/S0108270193012272
21. S. Thangarasu, V. Siva, S. Athimoolam and S.A. Bahadur, *Comput. Chem.*, **174**, 1850021 (2018); https://doi.org/10.1142/S0219633618500219
22. A.U. Alam, M. Khan, M. Alam and S. Ahmad, *J. Mol. Struct.*, **1178**, 570 (2019); https://doi.org/10.1016/j.molstruc.2018.10.063
23. A.V. Kulinich and A.A. Ishchenko, *Comput. Theor. Chem.*, **1154**, 50 (2019); https://doi.org/10.1016/j.comptc.2019.03.018
24. B. Gassoumi, H. Ghalla and R.B. Chaabane, *Heliyon*, **5**, e02822 (2019); https://doi.org/10.1016/j.heliyon.2019.e02822
25. H. Pir, N. Günay, Ö. Tamer, D. Avci and Y. Atalay, *Spectrochim. Acta A Mol. Biomol. Spectrosc.*, **112**, 331 (2013); https://doi.org/10.1016/j.saa.2013.04.063
26. G. Sivaraj, N. Jayamani and V. Siva, *J. Mol. Struct.*, **1216**, 128242 (2020); https://doi.org/10.1016/j.molstruc.2020.128242
27. V. Balachandran, A. Janaki and A. Nataraj, *Spectrochim. Acta A Mol. Biomol. Spectrosc.*, **118**, 321 (2014); https://doi.org/10.1016/j.saa.2013.08.091
28. N. Prabavathi, A. Nilufer and V. Krishnakumar, *Spectrochim. Acta A Mol. Biomol. Spectrosc.*, **114**, 449 (2013); https://doi.org/10.1016/j.saa.2013.05.011